Selective Quantum-Well Intermixing in GaAs–AlGaAs Structures Using Impurity-Free Vacancy Diffusion

Boon Siew Ooi, *Member, IEEE,* K. McIlvaney, Michael W. Street, Amr Saher Helmy, Stephen G. Ayling, *Member, IEEE,* A. Catrina Bryce, *Member, IEEE,* John H. Marsh, *Senior Member, IEEE,* and J. S. Roberts

***Abstract*— Impurity-free vacancy disordering (IFVD) using SiO_2 and SrF_2 dielectric caps to induce selective quantum-well (QW) intermixing in the GaAs–AlGaAs system is studied. The intermixing rate of IFVD was found to be higher in n-i-p and intrinsic than in p-i-n structures, which suggests that the diffusion of the Group III vacancy is not supported in p-type material. Single-mode waveguides have been fabricated from both as-grown and bandgap-tuned double-quantum-well (DQW) laser samples. Propagation losses as low as 8.5 dB·cm^{-1} were measured from the bandgap-tuned waveguides at the lasing wavelength of the undisordered material, i.e., 860 nm. Simulation was also carried out to study the contribution of free-carrier absorption from the cladding layers, and the leakage loss induced by the heavily p-doped GaAs contact layer. It was found that the leakage loss contributed by the GaAs cap layer is significant and increases with wavelength.**

Based on IFVD, we also demonstrate the fabrication of multiple-wavelength lasers and multichannel wavelength division multiplexers using the one-step "selective intermixing in selected area" technique. This technique enables one to control the degree of intermixing across a wafer. Lasers with bandgaps tuned to five different positions have been fabricated on a single chip. These lasers showed only small changes in transparency current, internal quantum efficiency, or internal propagation loss, which indicates that the quality of the material remains high after being intermixed. Four-channel wavelength demultiplexers based on a waveguide photodetector design have also been fabricated. Photocurrent and spontaneous emission spectra from individual diodes showed that the absorption edge was shifted by different degrees due to the selective degree of QW intermixing. The results obtained also imply that the technique can be used in the fabrication of broad-wavelength emission superluminenscent diodes.

***Index Terms*— Gallium arsenide, integrated optoelectronics, mode-locked lasers, quantum-well intermixing, quantum wells, semiconductor lasers.**

Manuscript received April 30, 1997. This work was supported by the Engineering and Physical Sciences Research Council (U.K.) and the Ministry of Defence under Grant GR/K45968.

B. S. Ooi was with the Department of Electronics and Electrical Engineering, University of Glasgow, Glasgow G12 8QQ, U.K. He is now with the School of Electrical and Electronic Engineering, Nanyang Technological University, Singapore 639798.

K. McIlvaney, M. W. Street, A. Saher Helmy, A. C. Bryce, and J. H. Marsh are with the Department of Electronics and Electrical Engineering, University of Glasgow, Glasgow G12 8QQ, U.K.

S. G. Ayling was with the Department of Electronics and Electrical Engineering, University of Glasgow, Glasgow G12 8QQ, U.K. He is now with the Defence Research Agency, Great Malvern, Worcestershire WR14 3PS, U.K.

J. S. Roberts is with the Department of Electronic and Electrical Engineering, University of Sheffield, Sheffield S1 3JD, U.K.

Publisher Item Identifier S 0018-9197(97)07081-4.

I. Introduction

THE ABILITY to control the bandgap across a III–V semiconductor wafer is a key requirement for the fabrication of monolithic photonic integrated circuits (PIC's). The absorption band edge of quantum-well (QW) structures needs to be controlled spatially across a wafer to allow the fabrication of integrated lasers, modulators, and low-loss waveguides. This control can be achieved by selective epitaxial growth [1], etching, and regrowth on a bulk material or postgrowth quantum-well intermixing (QWI) techniques, such as impurity-induced disordering (IID) and impurity-free vacancy disordering (IFVD) [2].

QWI using the IFVD technique is one of the simplest and most versatile ways of controlling the bandgap of the QW after growth, particularly in GaAs–AlGaAs structures. This technique uses a SiO_2 dielectric cap to induce outdiffusion of Ga atoms during annealing so generating group III vacancies in the underlying GaAs–AlGaAs material. Due to the concentration gradient between Ga in the QW and Al in the barriers, the group III vacancies promote the diffusion of Al into a buried GaAs QW and Ga into the barriers, and hence shift the QW bandgap to higher energy by partially intermixing the QW. Selective intermixing can be achieved by using a SiO_2 layer, as the intermixing source, and a SrF_2 layer as the intermixing inhibit layer. This technique is essentially impurity free, therefore QWI using IFVD can avoid degrading the electrical properties or increasing the optical loss by introducing free-carrier absorption. This technique has been used to fabricate PIC's such as extended cavity lasers and integrated waveguide modulators [3].

In this paper, we examine IFVD effects in p-i-n and n-i-p GaAs–AlGaAs QW structures. We also demonstrate that a variation of the IFVD technique can be used to control the bandgap energy spatially across a wafer using a single annealing step—selective intermixing in selected area (SISA). Low-loss single-moded waveguides have been fabricated in both as-grown and bandgap-tuned double-quantum-well (DQW) laser structures samples. The propagation losses in these two waveguides were measured and compared. Devices, such as SISA bandgap-tuned lasers, which can be used as wavelength division multiplexer (WDM) sources, and four-wavelength-channel waveguide photodetectors are demonstrated using the IFVD and SISA techniques.

II. Material Structure and Experimental Procedures

A GaAs–AlGaAs DQW laser structure was used in most of the experiments and devices described in this paper, unless specified otherwise. This structure was grown by metal-organic vapor phase epitaxy (MOVPE) and was of the form of a separate-confinement heterostructure (SCH) DQW laser. The DQW region was undoped and consisted of two 10-nm-wide GaAs QW's, separated by a 10-nm $Al_{0.2}Ga_{0.8}As$ barrier. The top and bottom $Al_{0.2}Ga_{0.8}As$ layers were 0.1 μm thick to complete the waveguide core. Both the upper (0.9 μm thick) and the lower (1.5 μm thick) cladding layers were made of $Al_{0.4}Ga_{0.6}As$ and doped to a concentration of 5×10^{17} cm^{-3} using carbon and silicon, respectively. The top contact epitaxial layer consisted of 0.1 μm of GaAs doped with 5×10^{18} cm^{-3} of zinc. This material gave a 77-K photoluminescence (PL) peak at about 810 nm and a lasing wavelength from a broad-area laser at around 860 nm.

Selective intermixing was achieved by patterning the control regions (i.e., the regions in which bandgap shifts were suppressed) with a 100-nm layer of SrF_2. These SrF_2 layers were deposited by evaporation and patterned by a lift-off process. A 200-nm-thick layer of SiO_2 was then deposited over the samples by plasma-enhanced chemical-vapor deposition (PECVD). The QWI step was carried out using a rapid thermal processor (RTP) in a nitrogen atmosphere. The samples were placed face down on a piece of fresh GaAs and another piece of GaAs was placed over the back to provide an As overpressure during annealing. PL measurements performed at 77 K were carried out to measure the bandgap after intermixing. An annealing temperature of around 925 °C for 30 s was usually used, giving a wavelength blue-shift of about 25 nm ($\sim$40 meV).

III. IFVD of GaAs–AlGaAs

QWI takes place when the group III matrix elements of GaAs–AlGaAs interdiffuse. According to the model proposed by Deppe and Holonyak [4], the intermixing rate is dependent upon the Fermi-level effect. In this model, the equilibrium vacancy concentration is found from simple thermodynamic considerations. The Al–Ga interdiffusion rate is then directly related to the concentration of group III vacancies and group III interstitials in the material.

The concentrations of charged point defects are determined by the position of the Fermi level. Of particular interest are the acceptor-like group III vacancies in n-type material and donor-like group III interstitials in p-type material. The intermixing rate in n-type QW structures is dominated by the diffusivity and concentration of group III vacancies under As-rich conditions. Similarly, in p-type QW structures, the QWI rate is determined by the diffusivity and concentration of group III interstitials under As-poor conditions.

In the case of IFVD, it is well known that Ga has a high diffusion coefficient in SiO_2 dielectric caps at annealing temperatures above 800 °C. Ga vacancies generated using this technique have been found to be responsible for a large IFVD effect in the GaAs–AlGaAs QW system [5].

A complete model of all of the factors which play a part in enhancing Ga outdiffusion into SiO_2 at elevated temperatures in the GaAs–AlGaAs system has not yet been developed. In addition to the high diffusion coefficient of Ga in SiO_2, Ga has a solubility limit in SiO_2 which may be dependent on the permeability (and hence on the deposition conditions) of the film. The other major factor is the thermal stress at the interface between the GaAs and the SiO_2 layer. The thermal expansion coefficient of GaAs is about ten times larger than that of SiO_2. During the annealing stage, the GaAs will be under tensile stress which the outdiffusion of Ga would help to relieve. The SiO_2 layers deposited using PECVD are highly porous and some of the bonding network of SiO_2 may be broken due to the stress gradient between the GaAs and SiO_2 films. This would enhance the diffusion of Ga atoms through the SiO_2 network. Arsenic atoms will also undoubtedly diffuse into the SiO_2 during high temperature annealing, however Ga atoms will outdiffuse preferentially as the diffusion coefficient of As in SiO_2 is extremely low compared to Ga [6]. At similar annealing temperatures, the effective diffusion rate of Ga has been found to be larger when using a short-rise-time RTP than using a conventional furnace [7], [8]. This observation suggests that stress induced at the SiO_2–GaAs interface is responsible for enhanced outdiffusion of Ga, as RTP causes greater stress at the SiO_2–GaAs interface than conventional furnace annealing. In addition, the intermixing rate of the IFVD process has been found to increase with increasing SiO_2 thickness [9]–[11]. This dependence on the thickness of the cap has been ascribed to the Ga concentration reaching its solubility limit in the SiO_2 cap. Once the solubility limit is reached, no more vacancies are generated, so thicker SiO_2 layers lead to more vacancies and hence to more intermixing. The experimental behavior is, however, also consistent with a stress-enhanced QWI rate, since a thicker SiO_2 film will induce a larger stress at the interface, therefore promoting more outdiffusion of Ga atoms and a larger intermixing rate.

In contrast to SiO_2, SrF_2 has a thermal expansion coefficient about three times higher than that of GaAs. The thermal stress induced at the SrF_2–GaAs interface during RTP is therefore lower in magnitude and opposite in sign to that at the SiO_2–GaAs interface. In addition, a relatively thin layer of SrF_2 has been used, which would also help to reduce the stress at the SrF_2–GaAs interface. These factors, together with the fact that the diffusion coefficient of Ga in SrF_2 is very much lower than in SiO_2, means that SrF_2 can be effectively used as an intermixing mask in IFVD to achieve selective intermixing in conjunction with SiO_2.

A. IFVD in n- and p-Type AlGaAs

As discussed above, the group III vacancy is negatively charged in GaAs. Hence, group III vacancies generated during IFVD should, in theory, result in different intermixing effects in intrinsic, p-doped and n-doped QW structures, if a similar As-partial pressure condition is used.

In this part of the experiment, we look at the effect of IFVD in intrinsic, p-i-n and n-i-p QW structures, as most practical photonic devices contain these layer structures. Wafers used in

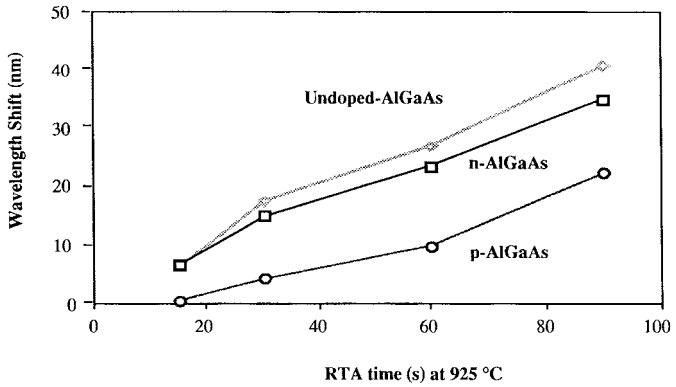

Fig. 1. Wavelength shifts as a function of annealing time obtained from SiO_2 capped intrinsic, n-i-p, and p-i-n samples annealed at 925 °C.

this experiment had a similar layer structure to the DQW laser material described above, apart from using semi-insulating substrates and the DQW region being replaced by a 200-nm single QW (SQW). In the case of n-i-p structures, the upper and lower cladding layers were n-doped and p-doped, respectively, instead of p-doped and n-doped in a usual p-i-n structure. The layers were left unintentionally doped for the intrinsic wafer. A 200-nm-thick SiO_2 film was deposited using PECVD on the samples and the annealing process was performed using an RTP at 925 °C for annealing times between 15 and 90 s.

The p-i-n and n-i-p wafers both have a similar degree of thermal stability [12], i.e., uncapped as-grown samples exhibited similar amounts of QWI after being annealed under similar RTP conditions. For samples capped with SiO_2, on the other hand, the undoped and n-i-p samples exhibit a larger degree of QWI than the p-i-n samples (Fig. 1). This may be attributed to the fact that the Ga vacancy is suppressed in p-type material and, therefore, smaller bandgap shifts were obtained. The n-doped contact and top cladding layer support Ga vacancies generated by the SiO_2 layer, hence larger degrees of intermixing were observed. From the point of view of fabricating PIC's, the above results suggest that the growth of n-i-p structures would give a higher degree of intermixing than the use of the conventional p-i-n structures typically used in QWI processes. These observations are in qualitative agreement with the QWI model proposed by Deppe and Holonyak [4].

The above results, however, conflict with the studies carried out by Seshadri *et al.* [13], who found that both p-i-n and n-i-p structures gave rise to similar amounts of QWI under similar processing conditions. Their experiment, however, was carried out by depositing the SiO_2 layer in direct contact with the AlGaAs layer rather than on a GaAs cap. When SiO_2 is in direct contact with AlGaAs, the Al can react with the SiO_2 to form Al_2O_3 and free Si. The Si atoms then diffuse through the semiconductor and into the QW, hence the QW is intermixed through the IID mechanism [3] rather than through IFVD. In addition, O atoms from the SiO_2 cap may also contribute a certain degree of intermixing in such conditions [14]. It is therefore believed that the combination of both IFVD and IID effects complicates analysis of the results.

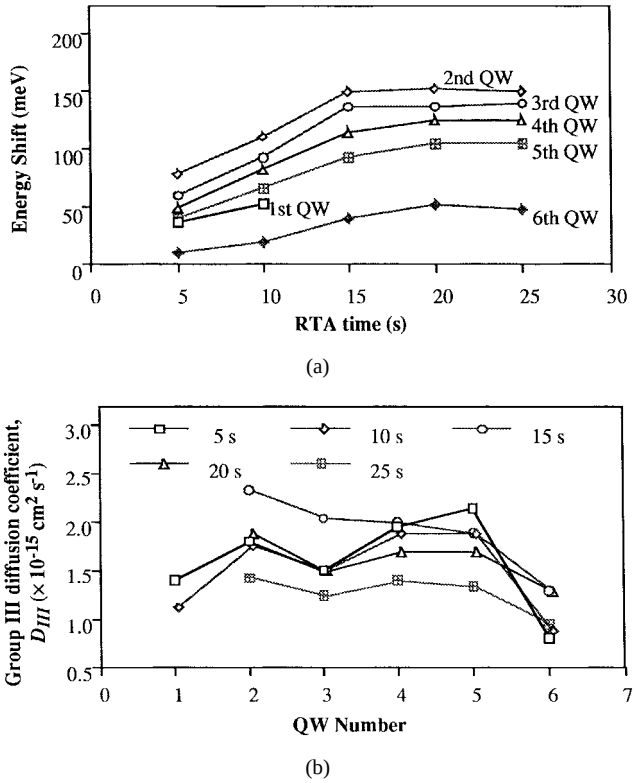

Fig. 2. (a) Bandgap shifts as a function of RTP time obtained from undoped MQW samples. The first QW is the narrowest QW, placed 300 Å below the surface, and the sixth QW is the widest and deepest QW, placed 0.45 μm from the surface. (b) Diffusion coefficients of the QW's corresponding to different anneal times.

B. Some Other Properties of Vacancies Generated by SiO_2

MQW samples were used to investigate the sensitivity of QW's with different well widths and at different depths to the diffusion of Ga vacancies. The other objective of this experiment was to study the depth dependence of the IFVD process.

The detailed structure of the sample used has been reported elsewhere [15]. In brief, this sample consisted of six undoped GaAs QW's with well widths of 25, 36, 43, 60, 70, and 95 Å, respectively, placed 300, 525, 761, 1005, 1265, 1535, and 4535 Å below the surface. RTP was carried out at 900 °C for annealing times between 5 and 20 s (with a rise time of 5 s). The bandgap shift as a function of annealing time for these six QW's is given in Fig. 2(a). These bandgap changes were then analyzed to give the effective diffusion coefficient for Ga–Al intermixing, D_{III} by using standard diffusion theory to model the shape of the partially intermixed well and then solving Schrödinger's equation using a shooting method algorithm [27]. A simple parabolic band structure was assumed and Adachi's data was used [20] for the electron, light, and heavy hole effective masses, and the electron and hole potentials as functions of the Al fraction. A value of D_{III} was chosen, the electron–hole transition energy was calculated, and then D_{III} was adjusted in an iterative manner until the calculated transition energy agreed with that observed experimentally. The diffusion coefficients are shown for different wells in Fig. 2(b).

It can be seen from Fig. 2(a) that the energy shift due to intermixing increases with decreasing well width, apart from the first QW, the narrowest QW, from which no PL could be resolved after annealing for 10 s, after which it is presumed that the well is completely disordered. The largest bandgap shift is, however, not observed from the first QW because it is only 25 Å thick; compared to wider QW's its quantized energy levels are closer to the valence and conduction bands in the barriers, and it is therefore less sensitive to QWI. This observation agrees with the findings of Koteles *et al.* [10].

The fact that the wells are of different widths means that the only meaningful way of assessing the variation of intermixing rate with depth is to look at D_{III}, the diffusion coefficient on the group III sites. Fig. 2(b) shows that D_{III} has a mean value of 2.5×10^{-15} $\mathrm{cm^2 s^{-1}}$ and is almost independent of well depth except possibly for the deepest well (depth of 4535 Å). The data also suggest that D_{III} is independent of time, except for 25-s anneal times when D_{III} is consistently low. This may be due to the SiO_2 layer becoming saturated with Ga atoms, therefore the degree of QWI does not increase linearly with RTP time.

C. SISA Process

Spatial control of the degree of bandgap energy shift across a wafer using most of the existing QWI techniques is indirect and complicated [11], [16], [17]. Based on IFVD, a simple one-step spatially controlled QWI technique, called selective intermixing in selected areas (SISA) has been developed [18]. In this process, the semiconductor is patterned with very small areas of SrF_2 followed by coating the sample with SiO_2. The degree of intermixing is then found to depend on the area of semiconductor surface in direct contact with the SiO_2 layer.

The SISA effect is achieved by patterning the semiconductor, using electron beam lithography, with submicron to 1 μm sized features of SrF_2 to act as a bandgap control mask, followed by deposition of SiO_2 over the samples to act as an intermixing source. The SrF_2 mask dimensions have to be smaller than, or comparable to, the diffusion length of the point defects to allow uniform intermixing at the QW depth by overlapping of the vacancy diffusion fronts (Fig. 3). From TEM work on MQW structures with similar composition, this diffusion length was found to be 3 μm for 1-μm-deep QW's, indicating a large diffusion constant and high mobility for the vacancies. As a result, spatial control of the bandgap shift can be achieved using a single RTP step. The degree of intermixing is dependent upon the area of sample in direct contact with the SiO_2 layer. This technique is simple, single-step, and reproducible.

The SISA technique was applied to a DQW laser structure. Six fields with size of 2 mm $\times$ 2 $\mathrm{mm^2}$ each containing 1 μm $\times$ 2 mm stripes of SrF_2 were defined in e-beam resist on top of the sample. SrF_2 was thermally evaporated onto the sample followed by lift-off. The SrF_2 area coverage studied varied between 8% and 50% (8%, 12%, 15%, 38%, 50%), which was achieved by varying the spacing between the 1-μm stripes. A 100% SrF_2 region was also prepared and the 0% reference was taken from the area outside the written fields. A layer of 200-nm SiO_2 was deposited by PECVD after the SrF_2 lift-off, and annealing was performed using an RTA at 925 °C for 30 s.

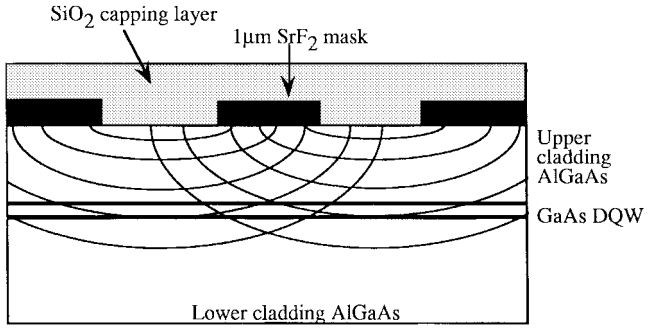

Fig. 3. Schematic representation of vacancy diffusion profile in SrF_2 masked QW material (not to scale). The high mobility of the vacancies leads to a uniform distribution at the DQW for patterns of a smaller dimension than the diffusion length (3 μm).

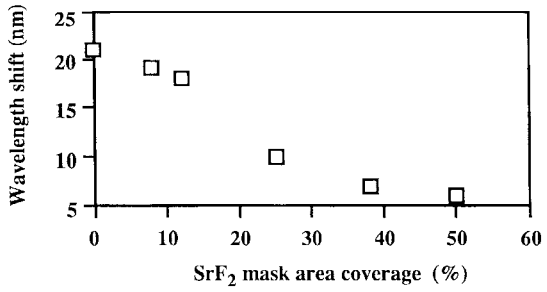

(a)

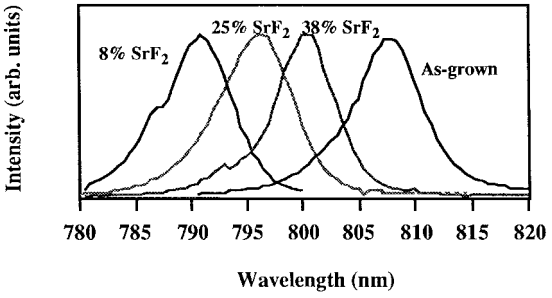

(b)

Fig. 4. (a) Wavelength shift and (b) 77-K PL spectra observed from the DQW material disordered using SISA technique.

PL measurements at 77 K were performed on these SISA intermixed fields. The bandgap shifts observed from the peak exciton are given in Fig. 4(a). Intermixing was inhibited in the 100% SrF_2 region [not shown in Fig. 4(a)]. Although the bandgap shift is not linear, it is observed that the degree of bandgap shift is dependent on the area coverage of the SrF_2. PL uniformity across the as-grown sample was better than 1 nm so we can be sure that the different wavelengths obtained were due to the intermixing process. Selected PL spectra of these measurements are given in Fig. 4(b). It is noted that the PL signals do not exhibit any significant broadening of their full width at half maximum (FWHM) and do not appear to be double peaked. This implies that the intermixing is even and homogeneous.

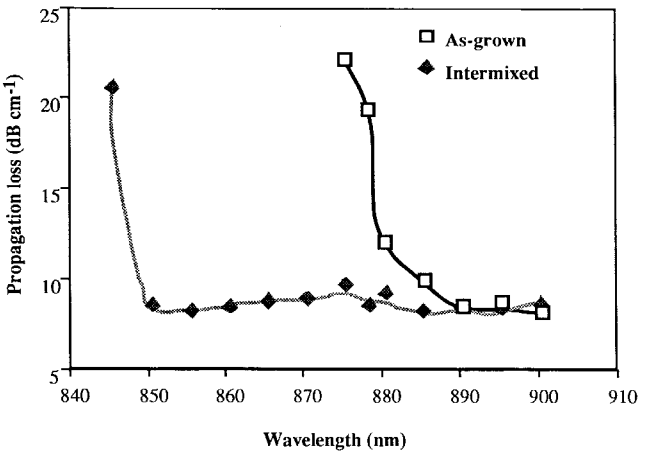

Fig. 5. Propagation loss as a function of wavelength measured from the as-grown and bandgap-tuned DQW samples.

IV. Devices

A. Low-Loss Waveguides

Single-moded ridge waveguides were fabricated from both as-grown DQW samples and samples with the bandgap tuned by 28 nm (i.e., 55 meV). These waveguides were 3 μm wide and dry etched to a depth of 0.8 μm to obtain single-mode guiding. The GaAs cap was selectively removed by wet-etching to prevent optical leakage loss into this GaAs cap. Propagation losses as a function of wavelength, measured using the Fabry–Perot technique, were carried out on cleaved 5-mm-long waveguides. Losses, from the as-grown and intermixed waveguides, as a function of wavelength in the range 840 to 900 nm, are given in Fig. 5.

In the case of the as-grown waveguides, the loss increases dramatically below a wavelength of 880 nm. The loss comes to a "floor" of around 9 dB·cm^{-1} above 890 nm. The intermixed waveguides, however, show a significant decrease in loss, allowing the measurement range to be extended to a wavelength as short as 850 nm. Since the bandgap has been shifted to higher energy, wavelengths which were strongly absorbed in the as-grown material now have become transparent in the partially intermixed samples. Losses as low as 8.5 dB·cm^{-1} have been observed in partially intermixed waveguides at the as-grown lasing wavelength of 860 nm. This loss is attributed mainly to the free-carrier absorption from the cladding layers and residual absorption from the material absorption tail at room tempreature, and partly to the scattering loss due to the imperfections incurred by the fabrication process. Apart from the shift in the position of the absorption edge, there are no significant changes in loss in the transparent wavelength region between the two sets of waveguides. The loss of 8.5 dB·cm^{-1} at 860 nm is 1.5 dB·cm^{-1} lower than that measured in the passive waveguides of extended cavity lasers fabrictated using a sample annealed at 900 °C for 30 s [22]. This is largely because the degree of intermixing of the studied waveguide is 11 nm higher than for the passive waveguides reported by Gontijo *et al.* [22], and the absorption tail at room temperature is therefore farther away from the lasing wavelength.

We extended the study to investigate the contribution of free-carrier absorption from both the p- and n-dopants in the AlGaAs cladding layers and the leakage loss into the GaAs cap layer using a computer simulation. A program for solving electromagnetic wave propagation in a waveguide using the finite difference method, called Fwave, was used for the simulation [19]. This software can be used to calculate the effective refractive index, the guiding conditions for different rib heights, and the two-dimensional (2-D) field distribution profiles for both TE and TM modes of a waveguide. The values of the refractive indices of GaAs–AlGaAs at the particular wavelengths and aluminum fractions used in this simulation were taken from Adachi [20].

Data obtained from the simulation consists of the electrical field distribution in arbitrary units, which is directly proportional to the square root of the power, in both the x and y directions. Supposing that the field distributed in the x direction is E_x and in the y direction is E_y, the total field E_{total} distributed in a waveguide can be found from

$$E_{\text{total}}^2 = E_x^2 + E_y^2. \tag{1}$$

The total intensity I_{total} of the guided light is directly proportional to the integrated square of the field, which can be expressed as

$$\int_{-\infty}^{+\infty} E_{\text{total}}^2 \cdot dx\, dy \propto I_{\text{total}}. \tag{2}$$

The optical overlap with a particular layer can therefore be written as

$$\Gamma_{\text{layer}(n)} = \frac{\int_{\text{layer}(n)} E_{\text{layer}(n)}^2 \cdot dx\, dy}{\int_{-\infty}^{+\infty} E_{\text{total}}^2 \cdot dx\, dy}. \tag{3}$$

The optical overlap with the cladding layers and the leakage loss into the GaAs cap layer are calculated from the interaction of light in the particular layer expressed as a fraction of the total intensity. The loss due to the free-carrier absorption in the cladding regions will be

$$\alpha_{\text{UC}} = C_{\text{UC}}\Gamma_{\text{UC}} \tag{4}$$

and

$$\alpha_{\text{LC}} = C_{\text{LC}}\Gamma_{\text{LC}} \tag{5}$$

where α_{UC} and α_{LC} are the losses due to the absorption from the holes and electrons from the upper and lower cladding layers, C_{UC} and C_{LC} are the loss coefficients, and Γ_{UC} and Γ_{LC} are the optical intensity overlaps with the upper and lower cladding layers, respectively. Data from the simulations show that the ratio Γ_{UC} varies from 0.1246 to 0.1433, and Γ_{LC} varies from 0.1380 to 0.1595 at wavelengths from 850 to 950 nm.

The free-carrier absorption coefficients, α_{fc}, for both n- and p-doped materials were calculated using the equation given below:

$$\alpha_{fc} \approx 7 \times 10^{18} \times P + 3 \times 10^{18} \times N \tag{6}$$

where P and N are the densities of holes and electrons, respectively, in cm^{-3}. This equation has been found to fit

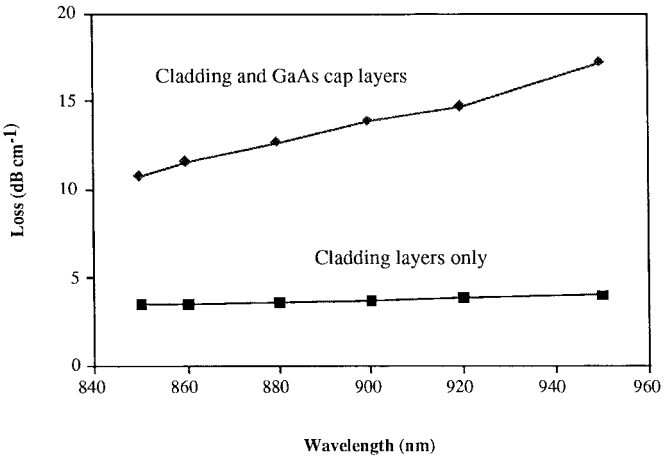

Fig. 6. Calculated absorption coefficient as a function of wavelength due to free carriers in the cladding layers and due to the GaAs cap layer.

various experimental data and is widely used [21]. In this analysis, we therefore take C_{UC} as 16.42 dB·cm^{-1} and C_{LC} as 10.03 dB·cm^{-1} for p- and n-doped with concentrations of 5.4×10^{17} cm^{-3} and 7.7×10^{17} cm^{-3}, respectively, using the equation above, and assume that C_{UC} and C_{LC} are constant throughout the range of wavelength studied. α_{UC} and α_{LC} are therefore found to change from 2.04 dB·cm^{-1} to 2.35 dB·cm^{-1} and 1.39 dB·cm^{-1} to 1.61 dB·cm^{-1} at wavelengths between 850 and 950 nm if the band edge absorption is not taken into account. The increase of loss with increasing wavelength is rather small and the loss can be considered to be constant within this range of wavelength. Summary results of $\alpha_{\mathrm{cladding}}$, where $\alpha_{\mathrm{cladding}} = \alpha_{\mathrm{UC}} + \alpha_{\mathrm{LC}}$, are given in Fig. 6.

Similarly, the loss due to radiation leakage into the GaAs cap region can be expressed

$$\alpha_{\mathrm{cap}} = C_{\mathrm{GaAs(cap)}} \Gamma_{\mathrm{GaAs(cap)}} \tag{7}$$

where $C_{\mathrm{GaAs(cap)}}$ is the loss coefficient of this layer. This coefficient includes the absorption due to heavy p-type doping (1.8×10^{19} cm^{-3}) and the radiation leakage resulting from the fact that the GaAs cap has a higher refractive index than that of the core guiding layer. From (6), the free-carrier absorption coefficient for this heavily p-doped layer is 547.22 dB·cm^{-1}. $\Gamma_{\mathrm{GaAs(cap)}}$ obtained from the simulation varies from 0.0134 to 0.0242, therefore the loss contributed by α_{cap} will sit in the range 7.33 dB·cm^{-1} to 13.24 dB·cm^{-1} in the wavelength range 850 to 950 nm (Fig. 6).

The propagation loss versus wavelength induced by free carriers in the cladding layers is given in Fig. 6. The loss obtained here is less than 4 dB·cm^{-1}, but the losses become significant if the radiation leakage into the GaAs cap region is taken into account. It is noted from Fig. 6 that the optical field overlapping with the cladding layer and absorbed by free carriers from the p- and n-dopant layers shows only a very small increase with increasing wavelength. However, if the leakage of the light into the cap region is considered, the loss toward the long wavelength region will increase gradually. These results suggest that the GaAs cap layer should be removed by etching in order to reduce the propagation loss of a waveguide. This is supported by the fact that losses as low as 3.6 dB·cm^{-1} have been measured in the passive waveguide sections of extended cavity lasers, in which the GaAs cap was removed from the passive sections (sample annealed at 950 °C for 30 s) [22].

B. SISA Lasers

The SISA technique is important in fabricating devices needed in applications such as WDM, in which a number of independent wavelengths are transmitted simultaneously via a single optical fiber. Such components are key for high-capacity information networks.

The fabrication of multiple wavelength lasers is described in this section. A 12 mm × 12 mm DQW sample was patterned with four different SrF_2 coverage fractions, 15%, 25%, 50%, and 100%. Each of the stripe patterned areas, which were ultimately to form the laser gain regions, measured 75 μm × 8 mm and they were spaced 300 μm apart. The sample was intermixed using the technique described above. After annealing, the SrF_2–SiO_2 layers were removed by wet etching in buffered HF and a new layer of 200 nm of SiO_2 was deposited. Oxide stripe bandgap–tuned lasers 75 μm wide were then fabricated on the SISA intermixed regions using standard photolithography techniques and wet-etching. The lasers were thinned and metal contacts were deposited on the n- and p-type surfaces. The lasers were then cleaved into different lengths from 300 to 900 μm.

The lasers were tested under pulsed conditions at room temperature. The current pulsewidth was 400 ns and the repetition frequency was 1 kHz (duty cycle 1:2500). An average of about eight lasers was measured for each of four different cavity lengths taken from six sets of lasers, five intermixed under different coverages of SrF_2 and one as-grown. Lasers fabricated on a single chip using these SISA patterns were observed to operate at five well-separated wavelengths (861, 855, 848, 844, and 840 nm) (Fig. 7), whilst the lasers fabricated from the as-grown material showed a lasing wavelength of 863 nm. These lasers were assessed thoroughly to determine the device quality after the SISA process [23]. The light–current characteristics were measured, and the threshold current and the slope efficiency were analyzed. A summary of the laser characteristics from samples intermixed to different degrees is tabulated in Table I. These lasers show only small changes in their infinite length threshold current density, and no correlation could be found between the degree of intermixing and the current density. The internal quantum efficiency of the intermixed material is a few percent lower than the as-grown material. However, these changes are very small, which indicates that the material quality has not been degraded by the SISA process. This technique is therefore useful in the production of WDM components, since the material produced by SISA is of high electrical and optical quality.

C. Four-Channel Waveguide Photodetectors

Two wavelength demultiplexers have previously been demonstrated using IFVD and other QWI related techniques [24], [25], [26]. In this section, we describe the use of the SISA

TABLE I
SUMMARY OF THE LASER CHARACTERISTICS FROM SAMPLES WITH DIFFERENT DEGREES OF INTERMIXING

SrF_2 coverage (%)	Threshold current density (for infinite length) (A cm^{-2})	Transparency current (A cm^{-2})	Internal quantum efficiency (%)	Loss (cm^{-1})
(as-grown)	218	62	71	14.7
0	227	62	68	14.5
15	235	64	68	14.5
25	251	68	66	14.0
50	217	60	64	12.1
100	237	63	65	12.0

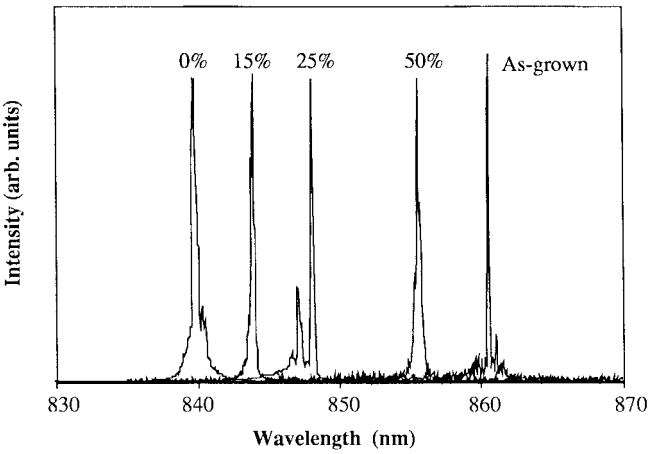

Fig. 7. The lasing spectra of lasers bandgap-shifted using the SISA technique.

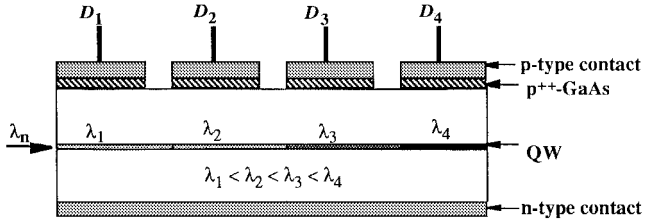

Fig. 8. Schematic cross section of the four-channel demultiplexing waveguide photodetector. The length of each diode is 300 μm and the spacing between diodes is 100 μm. Light was injected from the cleaved edge of diode D_1 during the photocurrent measurement.

technique to fabricate a four-channel waveguide photodetector. The device consists of four diodes, with bandgaps shifted by different degrees, placed in series along an optical waveguide. The intermixed regions serve both as absorbing layers for shorter wavelength light and as passive waveguides for the long wavelength light, so the longer wavelengths can pass into the diodes disordered to lower degrees. A schematic diagram of this device is shown in Fig. 8.

The SISA process was employed in the fabrication of this device. Four different SrF_2 coverage fractions, 0%, 25%, 50%, and 100%, were used. An annealing time of 60 s at 925 °C (30 s longer than for the SISA lasers) was used in order to obtain larger wavelength shifts and, hence, larger interchannnel wavelength spacings between the diodes. These intermixed regions were, again, realized by varying the spacing between 1-μm stripes within 300 μm $\times$ 5 mm bars, which were to form the diode regions. The spacing between the diodes was 100 μm and the diode length was 300 μm, long enough to absorb the optical signal. The p-type contact was defined using lift-off and the top p^+-GaAs layer between the electrodes was removed to improve electrical isolation. The sample was then thinned to about 180 μm and n-type metal contacts were evaporated. Devices were cleaved to a width of 300 μm for testing.

Waveguide photocurrents and spontaneous emission spectra were measured to assess the performance of these devices. The photocurrent measurements were carried out using an argon-ion pumped tunable Ti:sapphire laser whose output was end-fire coupled into the cleaved edge of the photodetector which had been intermixed to the largest degree (Fig. 8). Electrodes D_1, D_2, D_3, and D_4 denote diodes intermixed with SrF_2 coverages of 0%, 25%, 50%, and 100%, respectively, i.e., numbered with the absorption edge shifting from shorter to longer wavelength. During the measurements, adjacent diodes were grounded to prevent electrical interactions and the diode under test was reverse biased to -1.5 V. The photocurrent spectra measured from the individual diodes are given in Fig. 9. Fig. 9 suggests the optimum operating wavelengths for this device to be 832, 843, 855, and 868 nm for diodes D_1, D_2, D_3, and D_4, respectively. The number of channels can be easily extended using a similar technique if required.

The spontaneous emission spectra were measured from these diodes. A pulsed current, with parameters similar to those used for the SISA lasers, was injected into the diode to be measured whist the rest of the diodes were grounded. The emission spectrum was measured using a spectrum analyzer collecting the light at the cleaved edge of D_1. The spontaneous emission spectra are shown in Fig. 10(a). These spectra were measured under an injection current of 350 mA. Lasing, or stimulated emission, was observed from D_4 (100% SrF_2 coverage region) at injected current of around 500 mA, whilst only spontaneous emission was observed

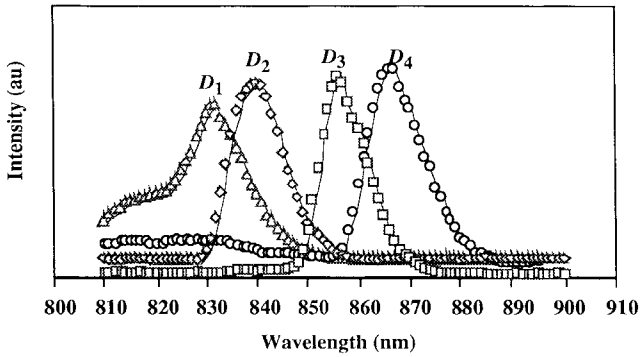

Fig. 9. Photocurrent spectra of diodes intermixed to different degrees. The injected light was unpolarized and the diodes were reverse biased to −1.5 V with adjacent diodes grounded during the measurements.

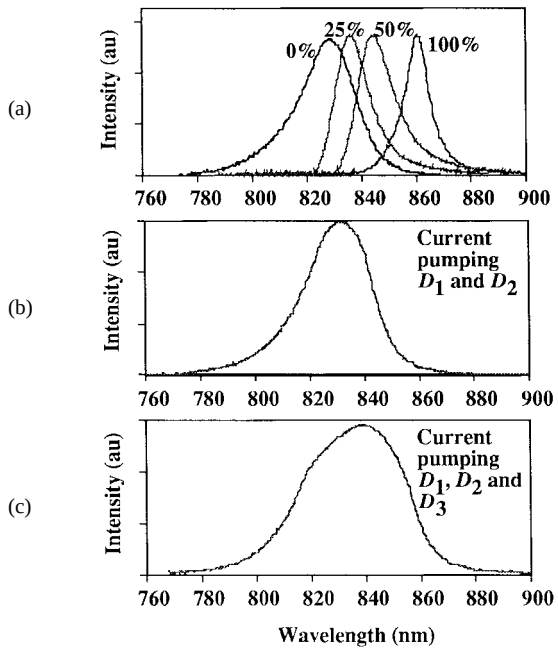

Fig. 10. (a) Spontaneous emission spectra from D_1, D_2, D_3, and D_4. The diodes were pumped with 350 mA. (b) Spectrum obtained from D_1 and D_2, whilst D_3 and D_4 were grounded. (c) Spectrum obtained from D_1, D_2, and D_3 whilst D_4 was grounded. All emission spectra were collected from the edge of diode D_1.

from D_1, D_2, and D_3. This is due to the fact that for D_4, the longest wavelength diode, the device acts as a broad-area extended cavity laser. In addition, D_4 absorbs short wavelength emission and suppresses the lasing mode of the other shorter wavelength diodes. The emission spectra are well spread, peaking at 828, 837, 847, and 861 nm for diodes D_1, D_2, D_3, and D_4, respectively. The peak positions are located at shorter wavelengths than the photocurrent spectra because the diodes were reverse bias during the photocurrent measurements.

From Fig. 10(a), it would appear that, as the degree of intermixing increases from D_4 to D_1, the degree of broadening to shorter wavelengths of the spontaneous emission spectra first reduces for D_3 and D_2 before increasing for the case of D_1. This phenomenon may be explained by calculating all of the interband transition wavelengths and oscillator strengths for intermixed coupled DQW potential profiles corresponding to the diodes D_1 to D_4. Again, standard diffusion theory was used to model the shape of the partially intermixed well and then Schrödinger's equation was solved to give the transition energies and the envelopes of the electron and hole wavefunctions. From the modeling results, it is possible to attribute the changes observed in the degree of broadening to shorter wavelengths of the diode spectra to the first bound electron to first bound light hole interband transition (e1→lh1): as the degree of intermixing increases from D_4 to D_1, the e1→lh1 transition wavelength first moves away from that of the corresponding e1→hh1 spontaneous emission peak wavelength before approaching it again for the case of the most intermixed diode D_1. (The e1→lh1/e1→hh1 wavelength separation is approximately 9 nm for D_4 compared to 6.5 nm for D_1.) In addition, the e1→lh1 oscillator strengths slowly increase relative to the corresponding e1→hh1 oscillator strength as intermixing proceeds. Hence, the reduced degree of broadening to shorter wavelengths of the D_3 and D_2 spontaneous emission spectra and the increased broadening to even shorter wavelengths of the D_1 spectrum relative to the spectrum of the least intermixed diode D_4, are mainly due to the presence of a significant e1→lh1 transition which initially diverges in wavelength from the e1→hh1 transition for diodes D_3 and D_2 before approaching it again for diode D_4.

The FWHM of the emission spectrum was found to increase from around 18 nm, when only D_1 is pumped, to 28 nm when D_1 and D_2 were electrically pumped with D_3 and D_4 grounded [Fig. 10(b)]. The FWHM of the spectrum was further increased to around 50 nm when D_1, D_2, and D_3 were pumped [Fig. 10(c)]. For this part of experiment, the pumping current was applied to all the diodes in parallel and totaled 1050 mA. These results demonstrate the use of the SISA technique to fabricate a broad-emission-spectrum superluminescent diode (SLD). The FWHM of the spectrum for such a device could be made broader if the degrees of intermixing in the absorbing regions were increased.

V. Summary and Conclusion

The IFVD technique has been demonstrated to be an effective method of controlling the bandgap spatially across a GaAs–AlGaAs QW wafer. The outdiffusion of Ga atoms is attributed partly to the high diffusion coefficient and the solubility of Ga in SiO_2 and to the interface stress induced by a large difference between the thermal expansion coefficients between SiO_2 and GaAs. From the studies carried out on intrinsic p-i-n and n-i-p structures, we confirmed that the diffusion of the group III vacancy is supported in n-type and intrinsic samples, but suppressed in p-type material.

Single-moded ridge waveguides have been fabricated from the as-grown and bandgap-tuned DQW samples. Propagation losses as low as 8.5 dB·cm^{-1} have been measured from the bandgap-tuned waveguides at a wavelength of 860 nm, i.e., the lasing wavelength of the as-grown material. Simulations have been carried out using a finite-difference electromagnetic program to study the contribution of free-

carrier absorption from the claddings, and the leakage loss into the GaAs cap layer to the total propagation loss. From the simulation results, it was found that loss due to radiation leakage into the GaAs cap layer is significant and increases with increasing wavelength. This implies that the heavily p-doped GaAs contact layer of a passive waveguide has to be removed by etching in order to obtain a low propagation loss.

A simple, one-step, and uniform spatially controlled QWI technique has been successfully used in the fabrication of bandgap-tuned lasers and four-channel waveguide photodetectors. Bandgap-tuned oxide stripe lasers, intermixed using this technique on a single chip, have been fabricated and five distinguishable lasing wavelengths have been observed. The quality of the material was shown to exhibit only small changes after intermixing. The technique was also used to fabricate four channel waveguide photodetectors. Both the photocurrent and spontaneous emission spectra were measured. The results showed that the devices can be operated as four-channel demultiplexing photodetectors at wavelengths determined during the SISA processing. The number of channels can be increased using the same technique. The SISA technique emerges as a promising technique in the fabrication of PIC's in III–V semiconductors.

REFERENCES

[1] M. Aoki, H. Sano, M. Suzuki, M. Takahashi, K. Uomi, and A. Takay, "Novel structure MQW electroabsorption modulator/DFB laser integrated device fabricated by selective area MOCVD growth," *Electron. Lett.*, vol. 27, pp. 2138–2140, 1991.

[2] See, for example, J. H. Marsh and A. C. Bryce, "Fabrication of photonic integrated circuits using quantum well intermixing," *Mater. Sci. Eng. B*, vol. 24, pp. 272–278, 1994.

[3] J. H. Marsh, P. Cusumano, A. C. Bryce, B. S. Ooi, and S. G. Ayling, "GaAs/AlGaAs photonic integrated circuits fabricated using impurity-free vacancy disordering," in *Proc. SPIE*, 1995, vol. 2401, pp. 74–85.

[4] D. G. Deppe and N. Holonyak, Jr., "Atom diffusion and impurity-induced layer disordering in quantum well III–V semiconductor heterostructures," *J. Appl. Phys.*, vol. 64, pp. R93–R113, 1988.

[5] D. G. Deppe, L. J. Guido, N. Holonyak, Jr., K. C. Hsieh, R. D. Burnham, R. L. Thornton, and T. L. Paoli, "Stripe-geometry quantum well heterostructure $Al_xGa_{1-x}As$-GaAs lasers defined by defect diffusion," *Appl. Phys. Lett.*, vol. 49, pp. 510–512, 1986.

[6] T. E. Haynes, W. K. Chu, and S. T. Picraux, "Direct measurement of evaporation during rapid thermal-processing of capped GaAs," *Appl. Phys. Lett.*, vol. 50, pp. 1071–1073, 1987.

[7] M. Katayama, Y. Tokuda, N. Ando, Y. Inoue, A. Usami, and T. Wada, "X-ray photoelectron spectroscopic study of rapid thermal processing on SiO_2/GaAs," *Appl. Phys. Lett.*, vol. 54, pp. 2559–2561, 1989.

[8] K. B. Kahen, D. L. Peterson, G. Rajeswaren, and D. J. Lawrence, "Properties of Ga vacancies in AlGaAs materials," *Appl. Phys. Lett.*, vol. 55, pp. 651–653, 1989.

[9] J. D. Ralston, S. O'Brian, G. W. Wicks, and L. F. Eastman, "Room-temperature exciton transitions in partially intermixed GaAs/AlGaAs superlattices," *Appl. Phys. Lett.*, vol. 52, pp. 262–264, 1988.

[10] E. S. Koteles, B. Elman, P. Melman, J. Y. Chi, and C. A. Armiento, "Quantum well shape modification using vacancy generation and rapid thermal annealing," *Opt. Quantum Electron.*, vol. 23, pp. S779–S787, 1991.

[11] J. Y. Chi, X. Wen, E. S. Koteles, and B. Elman, "Spatially selective modification of GaAs/AlGaAs quantum wells by SiO_2 capping and rapid thermal annealing," *Appl. Phys. Lett.*, vol. 55, pp. 855–857, 1989.

[12] B. S. Ooi, A. C. Bryce, J. H. Marsh, and J. S. Roberts, "Effect of p and n-doping on neutral impurity and SiO_2 dielectric cap induced quantum well intermixing in GaAs/AlGaAs structures," *Semicond. Sci. Technol.*, vol. 12, pp. 121–127, 1997.

[13] S. Seshadri, L. J. Guido, and P. Mitev, "Impurity-free layer disordering in p-i-n and n-i-p AlGaAs-GaAs multiple quantum well device structures: The Fermi level effect revisited," *Appl. Phys. Lett.*, vol. 67, pp. 497–499, 1995.

[14] L. J. Guido, J. S. Major, Jr., J. E. Baker, W. E. Plano, N. Holonyak, Jr., K. C. Hsieh, and R. D. Burham, "Column III vacancy- and impurity-induced layer disordering of $Al_xGa_{1-x}As$-GaAs heterostructures with SiO_2 or Si_3N_4 diffusion source," *J. Appl. Phys.*, vol. 67, pp. 6813–6818, 1990.

[15] B. S. Ooi, A. C. Bryce, C. D. W. Wilkinson, and J. H. Marsh, "Study of reactive ion etching-induced damage in GaAs/AlGaAs structures using a quantum well intermixing probe," *Appl. Phys. Lett.*, vol. 64, pp. 598–600, 1994.

[16] M. Ghisoni, R. Murry, A. W. Rivers, M. Pete, G. Hill, K. Woodbridge, and G. Parry, "An optical study of encapsulant thickness-controlled interdiffusion of asymmetric GaAs quantum well material," *Semicond. Sci. Technol.*, vol. 8, p. 1791–1794, 1993.

[17] M. Kuzuhara, T. Nozaki, and T. Kamejima, "Characterization of Ga out-diffusion from GaAs into SiO_xN_y films during thermal annealing," *J. Appl. Phys.*, vol. 66, pp. 5833–5836, 1989.

[18] S. G. Ayling, J. Beauvais, and J. H. Marsh, "Spatial control of quantum well intermixing in GaAs/AlGaAs using a one-step process," *Electron. Lett.*, vol. 28, pp. 2240–2241, 1992.

[19] M. R. S. Taylor, "FWAVE—A vector E-M solver," Univ. of Glasgow, Glasgow, Scotland, 1993.

[20] S. Adachi, "GaAs, AlAs, and $Al_xGa_{1-x}As$: Material parameters for use in research and device applications," *J. Appl. Phys.*, vol. 58, p. R1–R29, 1985.

[21] H. C. Casey, Jr., and M. B. Panish, *Heterostructure Lasers*. New York: Academic, 1978, pt. A.

[22] I. Gontijo, T. Krauss, R. M. De La Rue, J. S. Roberts, and J. H. Marsh, "Very low loss extended cavity GaAs/AlGaAs lasers made by impurity-free vacancy diffusion," *Electron. Lett.*, vol. 30, pp. 145–147, 1994.

[23] B. S. Ooi, S. G. Ayling, A. C. Bryce, and J. H. Marsh, "Fabrication of multiple wavelength lasers in GaAs/AlGaAs structures using a one-step spatially controlled quantum well intermixing technique," *IEEE Photon. Technol. Lett.*, vol. 7, pp. 944–946, 1996.

[24] B. C. Johnson, J. C. Campbell, R. D. Dupuis, and B. Tell, "2-wavelength disordered quantum-well photodetector," *Electron. Lett.*, vol. 24, pp. 181–182, 1988.

[25] T. Miyazawa, T. Kagawa, I. Iwamura, O. Mikami, and M. Naganuma, "Two-wavelength demultiplexing p-i-n GaAs/AlGaAs photodetector using partially disordered multiple quantum well structures," *Appl. Phys. Lett.*, vol. 55, pp. 828–830, 1989.

[26] A. N. M. M. Choudhury, P. Melman, A. Silletti, E. S. Koteles, B. Foley, and B. Elman, "Metal-semiconductor-metal demultiplexing waveguide photodetectors in InGaAs/GaAs quantum well structures by selective bandgap tuning," *IEEE Photon. Technol. Lett.*, vol. 3, pp. 817–819, 1991.

[27] D. P. Dave, "Numerical technique to calculate eigenenergies and eigenstates of quantum wells with arbitrary potential profile," *Electron. Lett.*, vol. 27, pp. 19–21, 1991.

Boon Siew Ooi (M'95) was born in Penang, Malaysia, in 1967. He received the first class honours B.Eng. and Ph.D. degrees from the University of Glasgow, Glasgow, Scotland, in 1992 and 1994, respectively. His Ph.D. dissertation was on the fabrication of GaAs–AlGaAs photonic integrated circuits.

He was subsequently a Post-Doctoral Research Assistant at the same university, working on III–V-based photonic integrated circuits before joining Nanyang Technological University, Singapore, as a Lecturer in July 1996. His research interests included optoelectronic integration using quantum-well intermixing and nanofabrication of III–V semiconductors.

K. McIlvaney, photograph and biography not available at the time of publication.

Michael W. Street was born in Belfast, Northern Ireland, in 1969. He received the M.Eng. degree in electrical and electronics engineering from Imperial College, University of London, England, in 1993, and the Ph.D. degree in electronics from the University of Glasgow, Glasgow, Scotland, in 1997. His doctoral research was concerned with quantum-well intermixing for the control of second-order nonlinear optical effects in GaAs–AlGaAs multiple-quantum-well waveguides.

He is currently working in the field of mode-locked semiconductor lasers for the generation and conversion of terahertz frequencies.

Amr Saher Helmy was born in Cairo, Egypt, in 1970. He received the B.Sc. degree in electronics and telecommunication engineering from Cairo University in 1993 and the M.Sc. degree in electronics and electrical engineering from the University of Glasgow, Glasgow, Scotland. He is currently working towards the Ph.D. degree at the University of Glasgow.

His main research interests include linear and nonlinear guided wave integrated optoelectronics using quantum-well intermixing.

In 1994, he was awarded a British Council scholarship to pursue his M.Sc. degree, and he was awarded the Francis Morrison prize for outstanding performance. His contribution in the NATO school "New Trends in Terahertz Technology" won the best student poster prize.

Stephen G. Ayling (M'94) received the B.Sc. degree in theoretical physics from the University of Durham, Durham, England, in 1984 and the Ph.D. degree in II–VI photoluminescence from the University of St. Andrews, St. Andrews, Scotland, in 1989.

He worked for five years as a Research Assistant at the Department of Electronics and Electrical Engineering at the University of Glasgow, Glasgow, Scotland, in the optoelectronics group. His research there concerned DFB and DBR lasers and quantum-well intermixing in AlGaAs. In 1996, he moved to the Defence Evaluation Research Agency at Malvern, England, where his research interests are optoelectronic-microwave devices and subsystem integration.

A. Catrina Bryce (M'91), for photograph and biography, see p. 937 of the June 1997 issue of this JOURNAL.

John H. Marsh (M'91–SM'91), for biography, see p. 937 of the June 1997 issue of this JOURNAL.

J. S. Roberts, photograph and biography not available at the time of publication.